Molecular Phylogenetics and Evolution 152 (2020) 106922

Contents lists available at ScienceDirect

Molecular Phylogenetics and Evolution

journal homepage: www.elsevier.com/locate/ympev

Short Communication

Multilocus species-delimitation in the *Xerotyphlops vermicularis* (Reptilia: Typhlopidae) species complex

P. Kornilios[a,*], D. Jablonski[b], R.A. Sadek[c], Y. Kumlutaş[d], K. Olgun[e], A. Avci[e], C. Ilgaz[d]

[a] Department of Biology, University of Patras, GR-26500 Patras, Greece
[b] Department of Zoology, Comenius University in Bratislava, 84215 Bratislava, Slovakia
[c] Biology Department, American University of Beirut, Bliss Street, 1107 2020 Beirut, Lebanon
[d] Department of Biology, Faculty of Science, Dokuz Eylül University, 35160 Buca, İzmir, Turkey
[e] Department of Biology, Faculty of Science and Arts, Aydın Adnan Menderes University, Aydın, Turkey

ARTICLE INFO

Keywords:
East Mediterranean
Middle East
Molecular systematics
Reptiles
Squamata
Typhlopidae

ABSTRACT

Scolecophidia (worm snakes) are a vertebrate group with high ecomorphological conservatism due to their burrowing lifestyle. The Eurasian or Greek blindsnake *Xerotyphlops vermicularis* is their only European representative, a species-complex with an old diversification history. However, its systematics and taxonomy has remained untouched. Here, we extend previous work that relied heavily on mitochondrial markers, following a multi-locus approach and applying several species-delimitation methods, including a Bayesian coalescence-based approach (STACEY). Four "species" delimitation analyses based on the mtDNA (ABGD, bGMYC, mPTP, parsimony networks) returned 14, 11, 9 and 10 clusters, respectively. By mitotyping twice as many specimens as before, we have a complete picture of each cluster's distribution. With the exception of the highly-divergent Levantine lineage, the three independent nuclear markers did not help with phylogenetic resolution, as demonstrated in haplotype networks, concatenated and species-trees, a result of incomplete lineage sorting. The prevailing model from the coalescence-based species-delimitation identified two species: the lineage from the Levant and all others. We formally recognize them as distinct species and resurrect *Xerotyphlops syriacus* (Jan, 1864) to include the Levantine blindsnakes. Finally, *X. vermicularis* and *X. syriacus* may represent species-complexes themselves, since they include high levels of cryptic diversity.

1. Introduction

Species are the fundamental units of biodiversity used in many biological disciplines such as biogeography, ecology and evolution, and applied fields such as conservation biology and management. Historically, morphological traits and characters have been used for the identification of species, but in recent years it has been the analysis of molecular markers that gained great attention for the discovery of species, especially cryptic ones. Additionally, the increased utilization of molecular and genetic data has been accompanied by advances in analytical methods and tools, referred to as "DNA-based species delimitation" (Carstens et al., 2013).

The field of molecular systematics can prove particularly helpful when studying species-limits for organisms that exhibit high morphological (and ecomorphological) conservatism. The Scolecophidia (worm snakes) are a largely understudied group of vertebrates with more than 400 species. They present extremely conserved morphology mainly due to their exclusively burrowing lifestyle, compared to all other snakes, the Alethinophidia (true snakes) which are ecologically and morphologically much more diverse (Miralles et al., 2018). Worm snakes are predominantly distributed in tropical and subtropical regions, with the Eurasian or Greek blindsnake *Xerotyphlops vermicularis* (Merrem, 1820) the only native European representative of the group. The Eurasian blindsnake, although currently recognized as one species, occupies a relatively large part of the geographic distribution of its family, the Typhlopidae (Supplementary Fig. S1), and it includes very high levels of genetic diversity (Kornilios et al., 2012). It represents a species-complex that has diverged from its sister-taxon *X. socotranus* (Boulenger, 1889) roughly during the Eocene-Oligocene transition (Kornilios et al., 2013), while the diversification within the complex has occurred during the early Miocene (Kornilios et al., 2012; Kornilios, 2017). The biogeographic history of the complex has been investigated in several studies with the use of molecular data (Kornilios et al., 2011; 2012; 2013; Kornilios, 2017) but it is still a work-in-progress, since

* Corresponding author.
E-mail address: korniliospan@yahoo.gr (P. Kornilios).

https://doi.org/10.1016/j.ympev.2020.106922
Received 28 April 2020; Received in revised form 21 July 2020; Accepted 3 August 2020
Available online 06 August 2020
1055-7903/

several phylogenetic relationships have not been resolved or are unstable, while most conclusions have been drawn from the analysis of mitochondrial (mtDNA) markers.

However, the systematics and taxonomy of the group has remained relatively untouched. In Kornilios et al. (2012), several highly-divergent mtDNA clades were identified by analysing 130 *X. vermicularis* specimens. These corresponded to 10 evolutionary significant units (ESUs), using statistical-parsimony networks and following Fraser and Bernatchez (2001). However, the resulting polytomies and sole use of mtDNA may have overestimated the number of ESUs or "species" within the complex. Later, in Kornilios (2017), some of the polytomies of the mtDNA phylogeny were resolved with the addition of more mtDNA markers but with the analysis of fewer samples. Although that study aimed at a better phylogeographic inference for the Eurasian blindsnake, three levels of divergence could be identified leading to three respective hypotheses for the number of potential "species" within the complex. The most conservative hypothesis includes two species: the first, named clade A in all aforementioned studies, is distributed in south Syria and Jordan (possibly also Israel, Lebanon and Egypt), while the second includes all remaining *X. vermicularis* populations, presenting a much larger distribution and a strong internal genetic structure. The second hypothesis recognizes a total of four species within the complex: clade A and three more species distributed in south-west Turkey (clade B), Cyprus (clade D) and the remaining populations. Finally, according to the third and least conservative hypothesis, seven potential species occur within the Eurasian blindsnake complex: clades A, B and D, with the addition of four species distributed west (clades G + K), east (clades I + H + M + E), south (clade F) and south-east (clade C) of the Amanos or Nur Mountains in south-central Turkey and north-west Syria (Fig. 1), with the east lineage having spread to the westernmost and easternmost parts of the blindsnake's range (Fig. 1). However, these working hypotheses that are based solely on observed levels of mtDNA divergence have not been tested with any other type of data or with species-delimitation tools. Finally, the morphological investigation of the samples we have at hand reveals that they do not differ with regard to all available meristic characters (scale counts) and body measurements, while the preservation of our samples in different mediums does not allow a safe comparison of scale measurements (e.g. length or width of certain head scales; see Kornilios et al., 2018 for a comparison of formalin-preserved to ethanol-preserved specimens).

The scope of this study is to extend previous work that relied heavily on mitochondrial markers, take advantage of molecular species-delimitation techniques and provide an updated taxonomy for the *X. vermicularis* species complex. For this purpose, we have analyzed twice as many specimens compared to our previous works, with a better targeted and more thorough geographical representation that fills several gaps in our sampling. Additionally, we followed a multi-locus approach by also including several independent nuclear markers (nDNA), and applied different species-delimitation methods and tools of modern molecular systematics, including coalescent based approaches. Many recent studies of east Mediterranean reptiles that used current molecular-taxonomy methods on multi-locus data, have uncovered new cryptic species, elevated subspecies to the species level or resurrected old ones (e.g. Sindaco et al., 2014; Kornilios et al., 2018; Jablonski et al., 2019). These studies, including the present one, can provide a better assessment of biodiversity levels and a more stable taxonomic framework for the implementation of conservation actions.

2. Material and methods

2.1. Taxon and DNA sampling

A total of 243 *X. vermicularis* samples (113 new) were sequenced for the mtDNA markers, while, after preliminary species-delimitation analyses, nDNA markers were sequenced for a subset of 65 samples representing all mtDNA clusters. Sampling localities are shown in Fig. 1 and specimen data (working codes, localities and GenBank Accession Numbers) are given in Supplementary Table S2.

The five target-loci were PCR-amplified and sequenced using conditions and primers described in Kornilios et al. (2012) and Kornilios et al. (2013); these were the mtDNA markers 12S rRNA (*12S*) and NADH dehydrogenase subunit 2 (*ND2*), and the nuclear protein-coding genes of the brain derived neurotrophic factor (*BDNF*), neurotrophin 3 (*NT3*) and prolactin receptor (*PRLR*). Heterozygous positions for the nuclear markers were phased using the Bayesian algorithm of Phase 2.1 (Stephens and Scheet, 2005) implemented in DnaSP 5.10 (Librado and Rozas, 2009), with 1,000 iterations after a burn-in of 100. All estimated

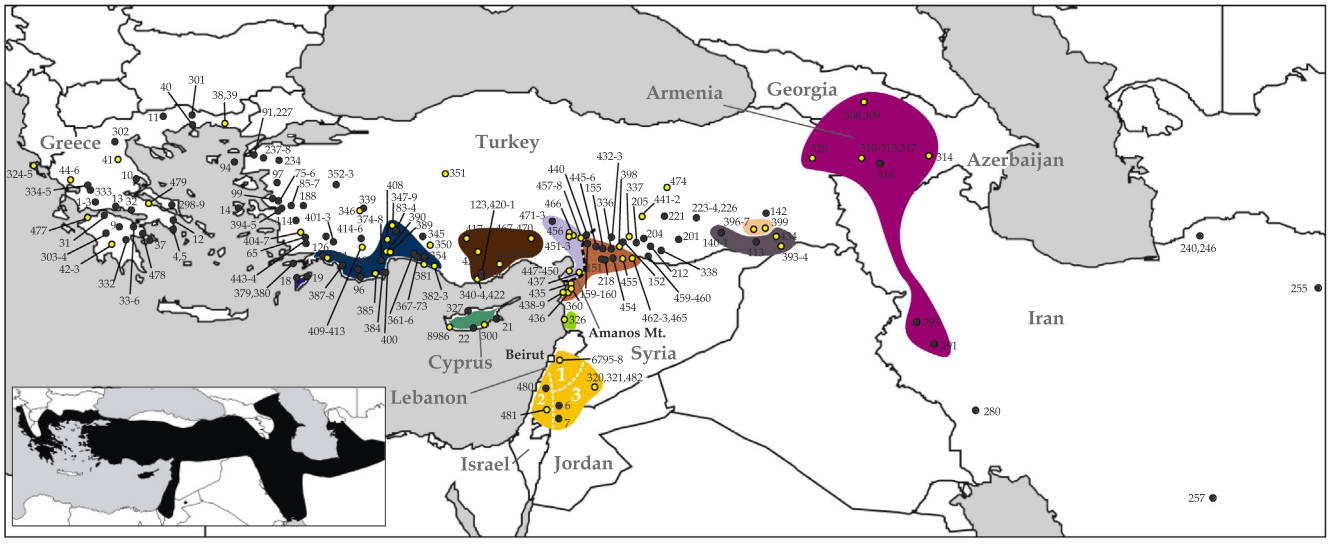

Fig. 1. Map showing the sampling localities of the current study: black circles for samples with mtDNA data and yellow circles for samples with mtDNA and nDNA data. The distribution of main phylogenetic clades is displayed with different colours that correspond to the clades of Fig. 1. All sampling localities that do not have a specific distribution-colour belong to the widespread clade I. Numbers refer to specimen codes given in the Supplementary Table S2. The geographic distribution of the *Xerotyphlops vermicularis* species complex is presented in the lower left inset (Sindaco and Jeremčenko, 2008). Finally, the names of important geographic areas and countries mentioned in the text are also presented. (For interpretation of the references to colour in this figure legend, the reader is referred to the web version of this article.)

haplotypes had probability values of 1.0. The genetic divergences between and within major mtDNA-groups were estimated using MEGA 6 (Tamura et al., 2013) as uncorrected *p*-distances.

2.2 Mitochondrial gene tree, single-locus species delimitation and haplotype networks

A Maximum Likelihood (ML) gene-tree was estimated for the mtDNA using IQ-TREE 1.4.3 (Nguyen et al., 2015). A free rate of heterogeneity was selected and nodal support was tested via SH-aLRT tests with 10,000 replicates (Guindon et al., 2010), 10,000 ultrafast bootstrap alignments (Minh et al., 2013) and 100 standard bootstraps (Felsenstein, 1985). During the analysis, the best partitioning scheme (one partition) and best substitution model (HKY + G), were also evaluated (Chernomor et al., 2016; Kalyaanamoorthy et al., 2017).

We applied several mtDNA-based species-delimitation analyses, inspired by the phylogenetic species concept and the DNA barcoding approach, that utilize different algorithms and tools, incorporating different theoretical backgrounds. Specifically, the Automatic Barcode Gap Discovery (ABGD; Puillandre et al., 2012) is a distance-based method, that can identify β-diversity relying on sequence similarity-thresholds but ignoring the relationships of the studied taxa. The Generalized Mixed Yule-Coalescent analysis (GMYC; Pons et al., 2006) and Poisson Tree Processes model (PTP; Zhang et al., 2013) are not distance-based and account for the phylogenetic relationships of the sequences. GMYC requires an ultrametric tree as input and uses absolute or relative ages to separate the branches into two processes (speciation and coalescence) and to differentiate within and between species. PTP directly uses substitutions to determine the transition from a between- to a within-species process by assuming that a two parameter model (one for speciation and one for coalescence) best fits the data. On the other hand, the multi-rate PTP (mPTP; Kapli et al., 2017), also accounts for different levels of intraspecific genetic diversity deriving from differences in the evolutionary history or sampling of each species, consistently yielding more accurate delimitations with respect to the actual taxonomy (Kapli et al., 2017).

We used the online version of ABGD (http://wwwabi.snv.jussieu.fr/public/abgd/), calculated *p*-distances and used the default priors for the relative gap width (1.5), *Pmin* (0.001) and *Pmax* (0.1). All analyses involved 50 steps and 20 bins of distance distribution.

We used the Bayesian version of GMYC (Reid and Carstens, 2012), bGMYC v.1.0.2 in R Studio, implementing 50,000 MCMC steps with 40,000 steps as burn-in and a thinning of 100 steps. As input, we used 1,000 posterior (ultrametric) trees of mtDNA haplotypes constructed with BEAST v1.10.4 (Drummond et al., 2012). Two independent runs were conducted with a chain length of $3*10^7$ iterations, under the uncorrelated longnormal relaxed clock approach with a Yule tree prior. TRACER v1.6 (Rambaut and Drummond, 2007) was used to check for convergence and adequate effective sample size (ESSs). Independent runs were combined using Logcombiner, discarding the first 25% of each run as burn-in, and the tree was summarized with TreeAnnotator. For the bGMYC analysis we used a conservative posterior-probability threshold of 0.5 to identify putative species, compared to higher values that could overestimate the species' number.

The ML mtDNA tree was used as input in mPTP: two independent analyses ran with 10^8 generations, a thinning of 10^4 and a burn-in of 10%. Again, we used a conservative posterior-probability threshold of 0.95 to identify speciation events.

Finally, we constructed independent haplotype networks with statistical parsimony, using TCS v.1.21 (Clement et al., 2000) under the 95% connection limit of parsimony. Independent mtDNA networks were considered distinct evolutionarily significant units (ESUs), following Fraser and Bernatchez (2001). Similarly, we constructed haplotype networks for each of the nuclear markers.

2.3. Multilocus coalescent-based species tree and species delimitation

Multilocus coalescent-based species delimitation can test alternative hypotheses of lineage divergence allowing for gene tree discordance under genetic drift (Fujita et al., 2012). To estimate a species tree and to test species' boundaries in this framework, we performed the Species Tree and Classification Estimation, Yarely – STACEY v.1.2.5 (Jones, 2017), in BEAST2 v.2.6.0 (Bouckaert et al., 2019). All 65 samples and all loci were included in the analysis (the two mtDNA genes were considered a single locus), and for species' assignments (minimal clusters) we used the maximum number of mtDNA clusters, as estimated from the combination of our single-locus species delimitation analyses (13 species). Two runs of 10^9 generations were conducted, with an uncorrelated longnormal relaxed clock and a Yule tree prior [CollapseHeight = 0.001; CollapseWeight = beta (1.1) around (0.1); bdcGrowthRate = lognormal (M = 4.6, S = 1.5); pop-PriorScale = lognormal (M = − 7, S = 2); relativeDeathRate = beta (1.1)].

For the species-delimitation analysis, we applied equal ploidy for the nDNA and mtDNA loci since this is considered a more robust approach that avoids disproportionate influence of mtDNA data (Busschau et al., 2019). We used SpeciesDelimitationAnalyser (Jones, 2015) to process output files and examine the clusters of species assignments.

Finally, we reconstructed a ML tree using the concatenated dataset (mtDNA and nDNA markers) in IQ-TREE, using the same parameters for the analysis and nodal support as for the mtDNA. We used five partitions, one for each marker, with their own best-fit substitution model (TN + G for ND2; K2P + I for 12S and the nuclear loci). For the phylogenetic analysis, heterozygous positions of the nuclear markers were coded according to the IUPAC ambiguity codes.

3. Results and discussion

3.1. MtDNA: gene-tree and clusters

The mitochondrial phylogeny within the *X. vermicularis* species complex has been a long standing issue: it presents a large number of highly divergent mtDNA lineages with many unresolved relationships due to a combination of soft and hard polytomies (Kornilios et al., 2011; 2012), while, even a multi-marker mtDNA dataset of more than 3,700 bp has failed to resolve some of them (Kornilios, 2017). The dense sampling of the present study with almost twice as many analyzed samples and the inclusion of unrepresented areas (and lineages) especially from Anatolia (Fig. 1), which is the diversification center of the complex, has returned a similar phylogenetic result of many mtDNA clades with ambiguous relationships (Fig. 2). However, by mitotyping a plethora of samples we have now an almost complete picture of each clade's geographic distribution (Fig. 1), while we have identified two new clades (K and M) that had been undetected.

The four single-locus cluster delimitation analyses, based on the mtDNA, returned relatively similar results with some differences regarding both the number of clusters and the appointment of samples into the clusters. Specifically, ABGD, bGMYC, mPTP and parsimony networks favored the occurrence of 14, 11, 9 and 10 clusters, respectively (Fig. 2; Supplementary Figure S3). According to all analyses, each of the clades B, C, E, F, G and K constitute different clusters. Three of the four analyses favoured clade D of Cyprus as one cluster, with ABGD, the most prone to splitting, showing it might be two. The monophyletic unit of clades IHM can be considered either as one cluster or as three, corresponding to the individual clades. Finally, the very divergent clade A was regarded either as one cluster in two of the analyses, or two clusters, splitting the Lebanon population (subclade A1) or even three clusters, further splitting the individuals from Israel (A2) from those of Jordan and south Syria (A3).

Conclusively, the most conservative outcome that keeps the species-splitting to a minimum, is the existence of at least nine mtDNA clusters within *X. vermicularis* corresponding to clades A, B, C, D, E, F, G, K and

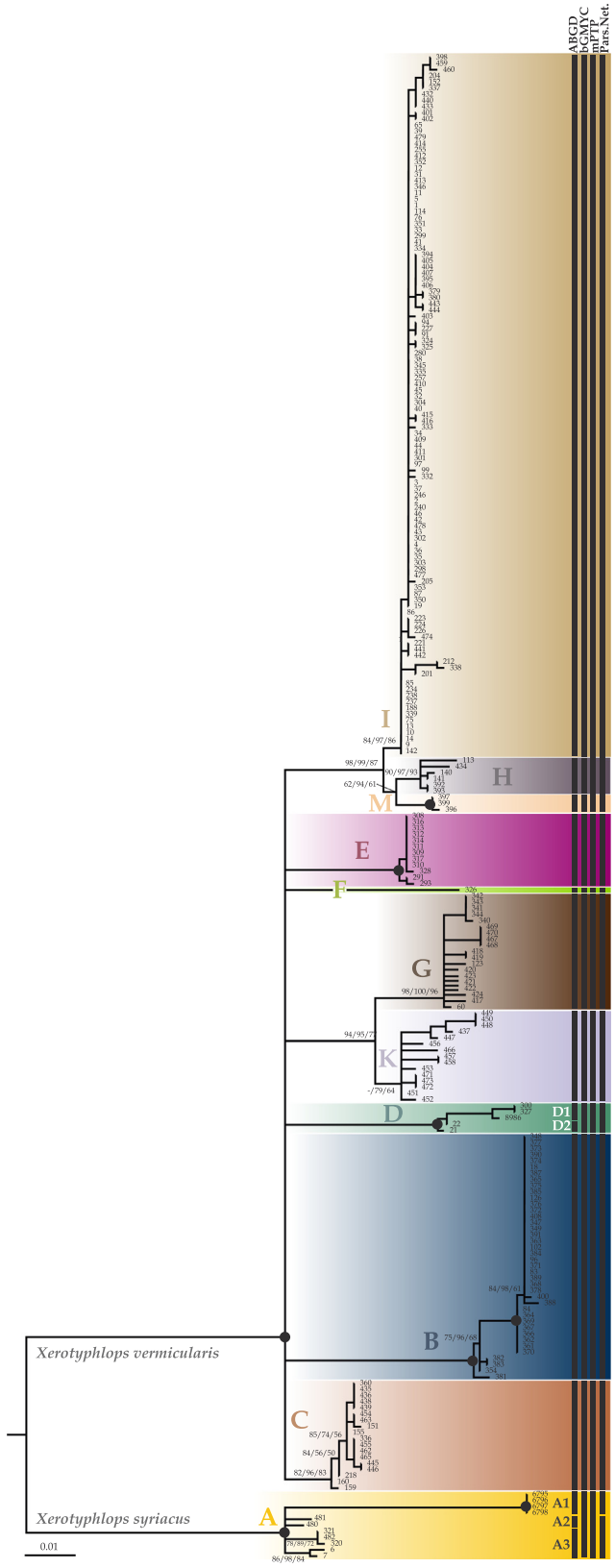

Fig. 2. Maximum Likelihood (ML) tree, reconstructed with IQ-TREE, based on the mtDNA dataset. Numbers in terminal nodes refer to specimen code numbers presented in Supplementary Table S2 and in the map of Fig. 1. Numbers next to nodes are statistical support values: SH-aLRT tests/ultrafast bootstrap alignments/standard bootstraps. Nodes with values ≤ 50 have been collapsed, while nodes with black closed circles indicate full support (100). Black vertical bars on the right of the clades are the results of the single-locus species-delimitation analyses (ABGD, bGMYC, mPTP, parsimony networks), with each segment representing a distinct candidate species according to the respective method.

the unit IHM. The maximum number of clusters, from the combination of all approaches, was 14 and was used in the coalescence-based species delimitation as the potential species, with the exception of D2 (samples 21, 22) due to failure in the PCR amplifications of the nuclear markers.

3.2. Multilocus coalescence-based species delimitation

Besides the clear separation of clade A, the analysis of three independent nuclear markers did not help with the phylogenetic resolution, as demonstrated in the independent networks (Fig. 3A) and the concatenated tree (Fig. 3B). In the species-tree, produced with STACEY (Supplementary Figure S4), all relationships were unsupported with the exceptions of the ancestor of clade A and the ancestor of all remaining clades that had a posterior probability value of 1.0. The observed patterns in the nuclear markers that are in conflict with the mtDNA, can be attributed either to introgression or to incomplete lineage sorting (ILS). We consider the former highly unlikely because if this is the case it would actually reflect a complete panmixia rather than local introgression and it would render the results from the mtDNA almost inexplicable.

STACEY returned a total of 145 different models for the number and composition of species within *X. vermicularis*. The prevailing one that is backed up by 80% of the posterior distribution of samples was the identification of two species, namely clade A and all others. Two other models were found in much smaller fractions of the distribution (6.5% and 5.7%); those were a single-species model and the recognition of a third species corresponding to clade D from Cyprus, respectively. All remaining 142 species-models covered less than 1% of the distribution each. As our nuclear-loci dataset is suffering from ILS, it becomes clear that the phylogeny and species-limits within the *X. vermicularis* complex will need a phylogenomic approach for their resolution, with the analysis of a large number of genomic markers and the added power of coalescence and population-genetics tools (work in progress).

For the time being and based on the current strong evidence, we are able to update and improve the systematic and taxonomic situation of the Eurasian blindsnake, by formally recognizing at least two valid species and identifying the populations of clade A as a distinct species from *X. vermicularis*.

3.3. The resurrection of Xerotyphlops syriacus and future work

The Italian zoologist, botanist and herpetologist Giorgio Jan (1791–1866) had described a blindsnake species from the area where we now find clade A (Jan, 1864). He named that species *Typhlops syriacus*, later synonymized with *T. vermicularis*, by describing a specimen found in Beirut, which is currently the capital of Lebanon but at that time was part of Syria. The sole specimen was unfortunately destroyed together with the entire collection of the Natural History Museum of Milan during the bombings of World War II (Scali, 2010). The samples from Lebanon included in our study come from a locality very close to Beirut, the type locality of *T. syriacus* (approximately 25 km west; Fig. 1). In this context, we resurrect the species *Xerotyphlops syriacus* (Jan, 1864) to formally include the populations belonging to our clade A, i.e. the Levantine blindsnake (Israel, Jordan, Lebanon, south Syria and probably Egypt). Although the original specimen is lost, a holotype still exists since Jan (1864) provided illustrations of the type specimen that should be designated as the holotype (Supplementary Figure S5). According to his brief morphological description of the single specimen from Beirut and a *X. vermicularis* representative from Cyprus, the main diagnostic character between them was the nasal furrow that did not surpass the nostril in the former while it did in the latter. The inspection

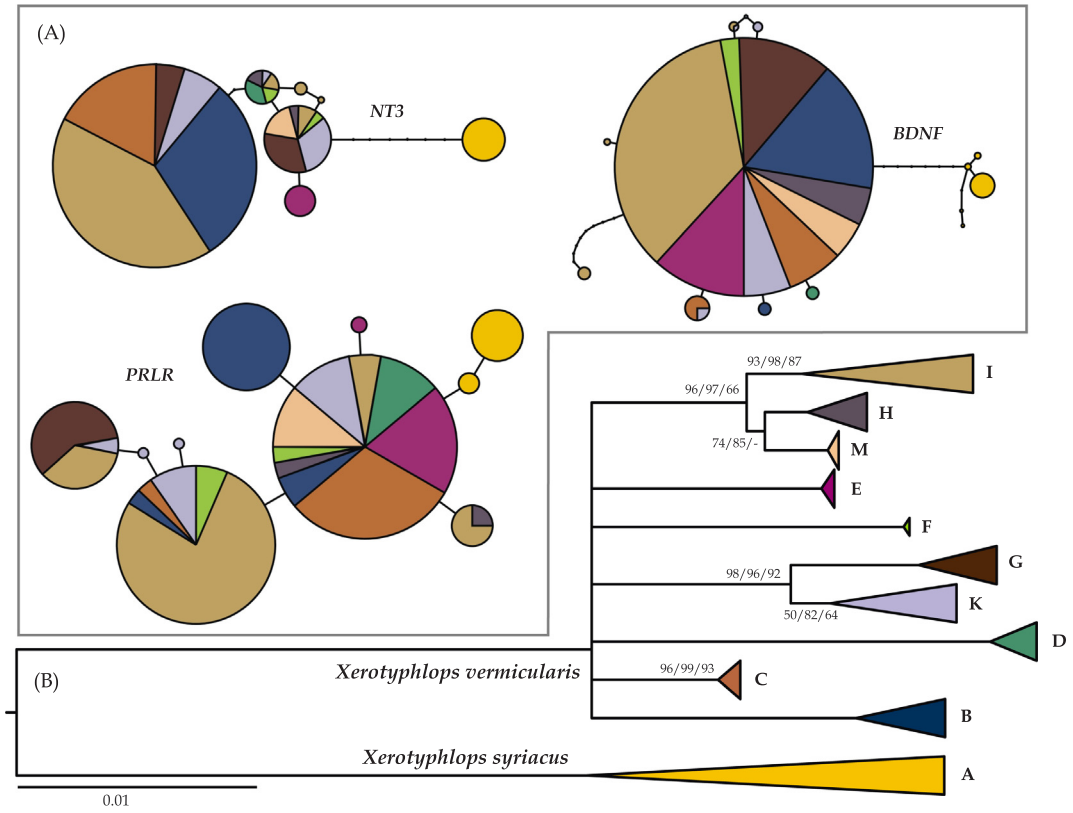

Fig. 3. (A) The statistical-parsimony networks based on the three nuclear markers (*NT3*, *BDNF*, *PRLR*) calculated with TCS with a 95% connection limit. Segment between black dots represents one mutational step, colored circles are haplotypes and colours refer to the clades of the mtDNA tree of Fig. 2. The circle area is proportional to the number of individuals sharing that haplotype. (B) The concatenated (mtDNA and nDNA) Maximum Likelihood (ML) tree, reconstructed with IQ-TREE. Branches of each clade have been collapsed (when not mentioned they have full statistical support, 100). Numbers next to nodes are statistical support values: SH-aLRT tests/ultrafast bootstrap alignments/standard bootstraps. Nodes with values ≤ 50 have been collapsed. (For interpretation of the references to colour in this figure legend, the reader is referred to the web version of this article.)

of our samples shows that this is not a character that differentiates the two species. A morphological investigation based on skeletal and cranial elements, using x-rays and ct-scans may prove more informative for the diagnosis of these two species, especially in the light of the extreme morphological conservatism that typhlopids and scolecophidians exhibit.

The evidence we have so far mostly from the mtDNA implies that both *X. vermicularis* and *X. syriacus* may represent species-complexes themselves, since they include high levels of cryptic diversity reflecting the existence of more species. The analysis of single-locus nuclear markers has not helped us confirm or reject this hypothesis, which will be tested with the use of genomic approaches and the analysis of introgression/hybridization levels between lineages. The genetic divergence values, as *p*-distances, between *X. vermicularis* and *X. syriacus* are very high, ranging from 10.6 to 13.0% for *ND2* and 4.4–5.7% for *12S* (Supplementary Table S6). However, the respective values among the intraspecific lineages of these two species are also high, comparable to or higher than species-level values from other reptiles (as high as 8.3% for *ND2* and 3.9% for *12S*; Table S3). Additionally, the mtDNA species-delimitation analyses recognize up to three "species" within *X. syriacus* and up to eleven "species" within *X. vermicularis* (Fig. 2). For the latter, the geographic distributions of these potential species coincide with known regions of high endemism and biodiversity (Kornilios et al., 2011; 2012; Jablonski and Sadek, 2019). For the former, according to some of our results, there are indications of genetic differentiation between populations from the north (Lebanon; A1), the west (Israel; A2) and the east (south Syria, Jordan; A3) that agree with known biogeographic barriers that have acted as speciation drivers in other organisms (Dufresnes et al., 2019 and references therein). However, a more thorough sampling is needed in order to evaluate the intraspecific diversity and taxonomic situation within *X. syriacus*.

CRediT authorship contribution statement

P. Kornilios: Conceptualization, Methodology, Validation, Formal analysis, Investigation, Resources, Data curation, Writing - original draft, Writing - review & editing, Visualization, Supervision, Project administration, Funding acquisition. **D. Jablonski:** Resources, Data curation, Writing - review & editing, Funding acquisition. **R.A. Sadek:** Resources, Writing - review & editing. **Y. Kumlutaş:** Resources, Data curation, Writing - review & editing, Funding acquisition. **K. Olgun:** Resources, Data curation, Writing - review & editing, Funding acquisition. **A. Avci:** Resources, Data curation, Writing - review & editing, Funding acquisition. **C. Ilgaz:** Resources, Data curation, Writing - review & editing, Funding acquisition.

Acknowledgements

We wish to acknowledge the people and institutions who donated samples for previous works that were also re-analyzed here: P. Lymberakis (Natural History Museum of Crete, Greece), J. Moravec (National Museum, Czech Rep.), R. Sindaco (Museo Civico di Storia Naturale di Carmagnola, Italy), C.L. Spencer (Museum of Vertebrate Zoology, University of California, Berkeley, USA) and N. Rastegar-Pouyani, M. Afroosheh (Department of Biology, Faculty of Science, Razi University, Iran). Tissue-samples from Israel were granted by the Steinhardt Museum of Natural History, Tel Aviv University. This research (PK) is co-financed by Greece and the European Union

(European Social Fund- ESF) through the Operational Programme "Human Resources Development, Education and Lifelong Learning" in the context of the project "Reinforcement of Postdoctoral Researchers – 2nd Cycle" (MIS-5033021), implemented by the State Scholarships Foundation (IKY). PK was also supported by the Committee for Research and Exploration of the National Geographic Society (Grant number 9260-13). We thank Daniel Gruľa for helping with fieldwork in Lebanon, Jana Polakova for laboratory work. DJ was supported by the Slovak Research and Development Agency under contract no. APVV-15-0147. The work (OK and AA) is part of two funded projects (Project No. TBAG-104 T294 — TBAG-108 T162) supported by TÜBITAK (The Scientific and Technical Research Council of Turkey).

Appendix A. Supplementary material

Supplementary data to this article can be found online at https://doi.org/10.1016/j.ympev.2020.106922.

References

Bouckaert, R., Vaughan, T.G., Barido-Sottani, J., Duchêne, S., Fourment, M., Gavryushkina, A., Heled, J., Jones, G., Kühnert, D., De Maio, N., Matschiner, M., Mendes, F.K., Müller, N.F., Ogilvie, H.A., du Plessis, L., Popinga, A., Rambaut, A., Rasmussen, D., Siveroni, I., Suchard, M.A., Wu, C.-H., Xie, D., Zhang, C., Stadler, T., Drummond, A.J., 2019. BEAST 2.5: An advanced software platform for Bayesian evolutionary analysis. PLoS Comput. Biol. 15 (4), e1006650.

Busschau, T., Conradie, W., Daniels, S.R., 2019. Evidence for cryptic diversification in a rupicolous forest-dwelling gecko (Gekkonidae: *Afroedura pondolia*) from a biodiversity hotspot. Mol. Phylogenet. Evol. 139, 106549.

Carstens, B.C., Pelletier, T.A., Reid, N.M., Satler, J.D., 2013. How to fail at species delimitation. Mol. Ecol. 22 (17), 4369–4383.

Chernomor, O., von Haeseler, A., Minh, B.Q., 2016. Terrace aware data structure for phylogenomic inference from supermatrices. Syst. Biol. 65, 997–1008.

Clement, M., Posada, D., Crandall, K.A., 2000. TCS: a computer program to estimate gene genealogies. Mol. Ecol. 9, 1657–1660.

Drummond, A.J., Suchard, M.A., Xie, D., Rambaut, A., 2012. Bayesian phylogenetics with BEAUti and the BEAST 1.7. Mol. Biol. Evol. 29, 1969–1973.

Dufresnes, C., Mazepa, G., Jablonski, D., Sadek, R.A., Litvinchuk, S.N., 2019. A river runs through it: tree frog genomics supports the Dead Sea Rift as a rare phylogeographical break. Biol. J. Linn. Soc. 128 (1), 130–137.

Felsenstein, J., 1985. Confidence limits on phylogenies: an approach using the bootstrap. Evolution 39, 783–791.

Fraser, D.J., Bernatchez, L., 2001. Adaptive evolutionary conservation: Towards a unified concept for defining conservation units. Mol. Ecol. 10, 2741–2752.

Fujita, M.K., Leaché, A.D., Burbrink, F.T., McGuire, J.A., Moritz, C., 2012. Coalescent-based species delimitation in an integrative taxonomy. Trends Ecol. Evol. 27 (9), 480–488.

Guindon, S., Dufayard, J.-F., Lefort, V., Anisimova, M., Hordijk, W., Gascuel, O., 2010. New algorithms and methods to estimate maximum-likelihood phylogenies: The performance of PhyML 3.0. Syst. Biol. 59, 307–321.

Jablonski, D., Kukushkin, O.V., Avcı, A., Bunyatova, S., Kumlutaş, Y., Ilgaz, Ç., Polyakova, E., Shiryaev, K., Tuniyev, B., Jandzik, D., 2019. The biogeography of *Elaphe sauromates* (Pallas, 1814), with a description of a new rat snake species. PeerJ 7, e6944.

Jablonski, D., Sadek, R.A., 2019. The species identity and biogeography of *Blanus* (Amphisbaenia: Blanidae) in Lebanon. Zool. Middle East 65 (3), 208–214.

Jan, G., 1864. Iconographie générale des ophidiens. 3. Livraison. Iconogr. gén. Ophid. 1 (3, livr.): 3.

Jones, G.R., 2015. Species delimitation and phylogeny estimation under the multispecies coalescent. bioRxiv.

Jones, G.R., 2017. Algorithmic improvements to species delimitation and phylogeny estimation under the multispecies coalescent. J. Math. Biol. 74, 447–467.

Kalyaanamoorthy, S., Minh, B.Q., Wong, T.K.F., von Haeseler, A., Jermiin, L.S., 2017. ModelFinder: fast model selection for accurate phylogenetic estimates. Nat. Methods 14 (6), 587–589.

Kapli, P., Lutteropp, S., Zhang, J., Kobert, K., Pavlidis, P., Stamatakis, A., Flouri, T., 2017. Multi-rate Poisson tree processes for single-locus species delimitation under maximum likelihood and Markov chain Monte Carlo. Bioinformatics 33 (11), 1630–1638.

Kornilios, P., 2017. Polytomies, signal and noise: revisiting the mitochondrial phylogeny and phylogeography of the Eurasian blindsnake species complex (Typhlopidae, Squamata). Zool. Scr. 46, 665–674.

Kornilios, P., Giokas, S., Lymberakis, P., Sindaco, R., 2013. Phylogenetic position, origin and biogeography of Palearctic and Socotran blind-snakes (Serpentes: Typhlopidae). Mol. Phylogenet. Evol. 68, 35–41.

Kornilios, P., Ilgaz, Ç., Kumlutas, Y., Giokas, S., Fraguedakis-Tsolis, S., Chondropoulos, B., 2011. The role of Anatolian refugia in herpetofaunal diversity: an mtDNA analysis of *Typhlops vermicularis* Merrem, 1820 (Squamata, Typhlopidae). Amphibia-Reptilia 32, 351–363.

Kornilios, P., Ilgaz, H., Kumlutas, Y., Lymberakis, P., Moravec, J., Sindaco, R., Rastegar-Pouyani, N., Afroosheh, M., Giokas, S., Fraguedakis-Tsolis, S., Chondropoulos, B., 2012. Neogene climatic oscillations shape the biogeography and evolutionary history of the Eurasian blindsnake. Mol. Phylogenet. Evol. 62, 856–873.

Kornilios, P., Kumlutaş, Y., Lymberakis, P., Ilgaz, Ç., 2018. Cryptic diversity and molecular systematics of the Aegean *Ophiomorus* skinks (Reptilia: Squamata), with the description of a new species. J. Zool. Syst. Evol. Res. 56, 364–381.

Librado, P., Rozas, J., 2009. DnaSP v5: a software for comprehensive analysis of DNA polymorphism data. Bioinformatics 25, 1451–1452.

Minh, B.Q., Nguyen, M.A., von Haeseler, A., 2013. Ultrafast approximation for phylogenetic bootstrap. Mol. Biol. Evol. 30, 1188–1195.

Miralles, A., Marin, J., Markus, D., Herrel, A., Hedges, S.B., Vidal, N., 2018. Molecular evidence for the paraphyly of Scolecophidia and its evolutionary implications. J. Evol. Biol. 31, 1782–1793.

Nguyen, L.T., Schmidt, H.A., von Haeseler, A., Minh, B.Q., 2015. IQTREE: A fast and effective stochastic algorithm for estimating maximum likelihood phylogenies. Mol. Biol. Evol. 32, 268–274.

Pons, J., Barraclough, T.G., Gomez-Zurita, J., Cardoso, A., Duran, D.P., Hazell, S., Kamoun, S., Sumlin, W.D., Vogler, A.P., 2006. Sequence-based species delimitation for the DNA taxonomy of undescribed insects. Syst. Biol. 55, 595–609.

Puillandre, N., Lambert, A., Brouillet, S., Achaz, G., 2012. ABGD, automatic barcode gap discovery for primary species delimitation. Mol. Ecol. 21, 1864–1877.

Rambaut, A., Drummond, A.J., 2007. Tracer v1.5. Available from http://tree.bio.ed.ac.uk/ software/tracer/.

Reid, N.M., Carstens, B.C., 2012. Phylogenetic estimation error can decrease the accuracy of species delimitation: a Bayesian implementation of the general mixed Yule-coalescent model. BMC Evol. Biol. 12, 196.

Scali, S., 2010. Storia e importanza scientifica della collezione erpetologica del Museo Civico di Storia Naturale di Milano, in Mazzotti, S., (Ed.), Le Collezioni Erpetologiche dei Musei Italiani: Censimento e Analisi delle Collezioni di Anfibi e Rettili per la Loro Valorizzazione Scientifica. Museologia Scientifica Memorie, Number 5, pp. 69–77.

Sindaco, R., Kornilios, P., Sacchi, R., Lymberakis, P., 2014. Taxonomic reassessment of *Blanus strauchi* (Bedriaga, 1884) (Squamata: Amphisbaenia: Blanidae), with the description of a new species from south-east Anatolia (Turkey). Zootaxa 3795, 311–326.

Sindaco, R., Jeremčenko, V.K., 2008. The reptiles of the Western Palearctic. Vol 1. Annotated checklist and distributional atlas of the turtles, crocodiles, amphisbaenians and lizards of Europe, North Africa, Middle East and Central Asia. Monografie della Societas Herpetologica Italica - I. Edizioni Belvedere, Latina, Italy.

Stephens, M., Scheet, P., 2005. Accounting for decay of linkage disequilibrium in haplotype inference and missing data imputation. Am. J. Hum. Genet. 76, 449–462.

Tamura, K., Stecher, G., Peterson, D., Filipski, A., Kumar, S., 2013. MEGA6: Molecular Evolutionary Genetics Analysis version 6.0. Mol. Biol. Evol. 30, 2725–2729.

Zhang, J., Kapli, P., Pavlidis, P., Stamatakis, A., 2013. A general species delimitation method with applications to phylogenetic placements. Bioinformatics 29, 2869–2876.

Supplementary Material

Multilocus species-delimitation in the *Xerotyphlops vermicularis* (Reptilia: Typhlopidae) species complex

Kornilios, P.; Jablonski, D.; Sadek, R.A.; Kumlutaş, Y.;Olgun, K., Avci, A.; Ilgaz Ç.

Figure S1. Map showing the geographic distribution of the family Typhlopidae (red) and the *Xerotyphlops vermicularis* species complex (yellow) (Vitt and Caldwell, 2014).

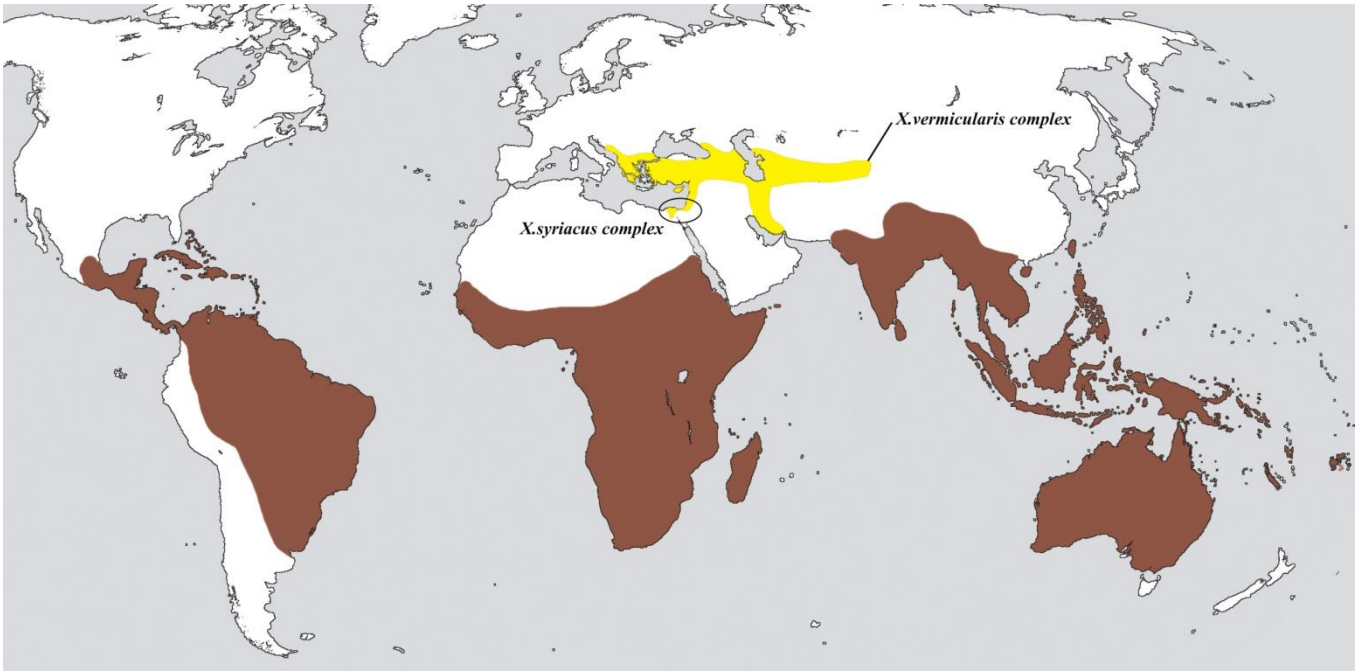

Table S2. Sample working codes and sampling localities (see map of Figure 1) of the specimens used in the phylogenetic analyses. GenBank accession numbers of sequence data for all DNA segments are also shown, with sequences JQ045130-JQ045275 from Kornilios et al. (2012) and all other sequences from the current study.

Museum abbreviations for the tissue-grants are as follows:

NHMC: Natural History Museum of Crete, Greece

ZDEU: Zoology Department, Ege University, Turkey

RUZM: Razi University Zoological Museum, Iran

MVZ: Museum of Vertebrate Zoology, Berkeley, USA

MCC: Museo Civico di Storia Naturale di Carmagnola, Italy

NPM6V: National Museum, Prague, Czech Republic

AAMU: Aydın Adnan Menderes University Museum Collection, Turkey

TAU-R: Steinhardt Museum of Natural History, Tel Aviv University, Israel

CUB: Comenius University in Bratislava, Department of Zoology, Slovakia

Code	Museum code	Locality (Country)	GenBank Accession Numbers				
			12S	ND2	BDNF	NT3	PRLR
1		Marathias to Thermo (Greece)	JQ045130	JQ045197			
2		Marathias to Thermo (Greece)	JQ045130	JQ045197			
3		Marathias to Thermo (Greece)	JQ045131	JQ045198			
4		Zagani hill, Spata (Greece)	JQ045132	JQ045199			
5		Zagani hill, Spata (Greece)	JQ045133	JQ045200			
6	NHMC 80.3.21.6	Ajloun (Jordan)	JQ045134	JQ045201			
7	NHMC 80.3.21.7	Zai Park (Jordan)	JQ045135	JQ045202			
9	NHMC 80.3.21.3	Stymfalia Lake (Greece)	JQ045137	JQ045203			
10	NHMC 80.3.21.15	Alykes, Volos (Greece)	JQ045138	JQ045204			
11	NHMC 80.3.21.16	Paranesti to Prasinada (Greece)	JQ045133	JQ045200			
12	NHMC 80.3.21.17	Agia Marina (Greece)	JQ045130	JQ045197			
13	NHMC 80.3.21.19	Elaia (Greece)	JQ045138	JQ045204			
14	NHMC 80.3.21.10	Mesta, Chios Isl. (Greece)	JQ045137	JQ045203			
18	NHMC 80.3.21.9	Artamity monastery, Rhodos Isl. (Greece)	JQ045140	JQ045206			
19	NHMC 80.3.21.1	Maritsa, Rhodos Island (Greece)	JQ045141	JQ045207			
21	NHMC 80.3.21.20	Greko cape (Cyprus)	JQ045142	JQ045208			
22	NHMC 80.3.21.12	Kyvernitis beach (Cyprus	JQ045143	JQ045209			
31		Platani (Greece)	JQ045144	JQ045210			
32		Galaxidi (Greece	JQ045130	JQ045197			
33		Akrokorinthos (Greece)	JQ045130	JQ045197			
34		Akrokorinthos (Greece)	JQ045130	JQ045197			
35		Akrokorinthos (Greece)	JQ045130	JQ045197			
36		Akrokorinthos (Greece)	JQ045145	JQ045211			
37		km N of Koliaki (Greece	JQ045146	JQ045212			
38		Makri (Greece)	JQ045130	JQ045197	MT773913	MT773978	JQ045263
39		Makri (Greece)	JQ045130	JQ045197			
40		Galani, Nestos (Greece)	JQ045130	JQ045197			
41		Tempi (Greece)	JQ045130	JQ045197	MT773914	MT773979	JQ045263
42		2 km N of Petrina (Greece)	JQ045130	JQ045197	MT773915	MT773980	MT774043
43		2 km N of Petrina (Greece)	JQ045130	JQ045197			
44		Zirou Lake (Greece)	JQ045130	JQ045197	MT773916	MT773981	JQ045263
45		Zirou Lake (Greece)	JQ045130	JQ045197			
46		Zirou Lake (Greece)	JQ045130	JQ045197			
60	ZDEU 131/1995/27A	Uzuncaburç, Silifke, Mersin (Turkey)	JQ045147	JQ045213			
65	ZDEU 168/2001/49A	Tire, İzmir (Turkey)	JQ045130	JQ045197			
75	ZDEU 307/1997/33F	Örnekköy, İzmir (Turkey)	JQ045148	JQ045214			

76	ZDEU 307/1997/33C	Örnekköy, İzmir (Turkey)	JQ045130	JQ045197			
83	ZDEU 49/1990/ 80A	Kovada, Isparta (Turkey)	JQ045149	JQ045215			
84	ZDEU 49/1990/80B	Kovada, Isparta (Turkey)	JQ045150	JQ045216			
85	ZDEU122/2008/ 77A	Yamaklar, İzmir (Turkey)	JQ045141	JQ045207			
86	ZDEU 122/2008/77B	Yamaklar, İzmir (Turkey)	JQ045141	JQ045207			
87	ZDEU 122/2008/77C	Yamaklar, İzmir (Turkey)	JQ045151	JQ045217			
91	ZDEU C46/2008-1	Çanakkale (Turkey)	JQ045152	JQ045218			
94	ZDEU C22/2008-1	Bozcaada Island, Çanakkale (Turkey)	JQ045153	JQ045219			
96	ZDEU D3/2009-1	Tersane Cove, Kekova, Kaş, Antalya (Turkey)	JQ045140	JQ045206			
97	ZDEU D1/2009-1	Bergama, İzmir (Turkey)	JQ045130	JQ045197			
99	ZDEU D5/2009-1	Emiralem, İzmir (Turkey)	JQ045154	JQ045220			
102	ZDEU D2/2009-1	Kale, Kaş, Antalya (Turkey)	JQ045140	JQ045206			
113	ZDEU C15/2008-1	Çığır, Şırnak (Turkey)	JQ045155	JQ045221			
114	ZDEU D4/2009-1	Buca, İzmir (Turkey)	JQ045130	JQ045197			
123	ZDEU 155/1999-1/41B	Zeyne, Mut, Mersin (Turkey)	JQ045156	JQ045222			
126	ZDEU 248/1991/14B	Çandır, Köyceğiz, Muğla (Turkey)	JQ045140	JQ045206			
140	ZDEU 124/2005/62A	17 km NW of Mardin (Turkey)	JQ045157	JQ045223			
141	ZDEU 124/2005/62B	17 km NW of Mardin (Turkey)	JQ045158	JQ045224			
142	ZDEU 213/2005/65A	Siirt (Turkey)	JQ045159	JQ045225			
151	ZDEU 42/2005/55A	Öncüpınar, Kilis (Turkey)	JQ045160	JQ045226			
152	ZDEU 60/2005/57A	16 km NW of Birecik / Şanlıurfa	JQ045130	JQ045197			
155	ZDEU70/2006/70A	4 km E of Polateli , Kilis (Turkey)	JQ045161	JQ045227			
159	ZDEU 78/2006/72B	Zincirlihöyük, Islahiye, Gaziantep (Turkey)	JQ045162	JQ045228			
160	ZDEU 78/2006/72C	Zincirlihöyük, Islahiye, Gaziantep (Turkey)	JQ045163	JQ045229			
188	ZDEU 307/1997/33B	Örnekköy, İzmir (Turkey)	JQ045148	JQ045214			
201	ZDEU91/2005/ 60A	32 km NE of Şanlıurfa (Turkey)	JQ045164	JQ045230			
204	ZDEU 45/2001/45A	Bağpınar, Adıyaman (Turkey)	JQ045165	JQ045231			
205	ZDEU 51/2006/68A	EskiSavaşan, Halfeti, Şanlıurfa (Turkey)	JQ045166	JQ045232			
212	ZDEU 84/2005/59C	Küçükalanlı, Şanlıurfa (Turkey)	JQ045167	JQ045233			
218	ZDEU 50/2005/56A	Kemaliye, Kilis (Turkey)	JQ045168	JQ045234			
221	ZDEU 54/2001/46B	Karadut, Kahta, Adıyaman (Turkey)	JQ045169	JQ045235			
223	ZDEU 135/2005/63A	48 km W of Diyarbakır (Turkey)	JQ045170	JQ045236			
224	ZDEU 135/2005/63B	48 km W of Diyarbakır (Turkey)	JQ045170	JQ045236			
226	ZDEU 135/2005/63D	48 km W of Diyarbakır (Turkey)	JQ045170	JQ045236			
227	ZDEUC46/2008-2	Çanakkale (Turkey)	JQ045153	JQ045219			
234	ZDEU C109/2007-7	Karaköy, Çanakkale (Turkey)	JQ045148	JQ045214			
237	ZDEU C45/2007-4	Kirazlı, Çanakkale (Turkey)	JQ045171	JQ045237			
238	ZDEU C45/2007-3	Kirazlı, Çanakkale (Turkey)	JQ045171	JQ045237			
240	RUZM 240	Gorgan (Iran)	JQ045130	JQ045197			
246	RUZM 246	Gorgan (Iran)	JQ045130	JQ045197			
255	RUZM 255	Neyshabur (Iran)	JQ045172	JQ045238			
257	RUZM 257	Sirjan (Iran)	JQ045172	JQ045238			
280	RUZM 280	Dezful (Iran)	JQ045172	JQ045238			
291	RUZM 291	Kermanshah (Iran)	JQ045173	JQ045239			
293	RUZM 293	Ravansar (Iran)	JQ045174	JQ045240			
298		Koutoumoulas, Evvoia Island (Greece)	JQ045130	JQ045197			
299		Koutoumoulas, Evvoia Island (Greece)	JQ045130	JQ045197			
300	NHMC 80.3.21.21	Lefkara (Cyprus)	JQ045175	JQ045241	MT773917	MT773982	MT774044
301	NHMC 80.3.21.22	Stavroupoli (Greece)	JQ045130	JQ045197			
302	NHMC 80.3.21.24	Prodromos monastery, Aliakmonas (Greece)	JQ045130	JQ045197			
303		8 km S of Labia (Greece)	JQ045130	JQ045197			
304		8 km S of Labia (Greece)	JQ045130	JQ045197			
308	MVZ 218698	Southern hills of Tbilisi (Georgia)	JQ045176	JQ045242			
309	MVZ 218699	Southern hills of Tbilisi (Georgia)	JQ045176	JQ045242	MT773918	MT773983	JQ045263
310	MCC R1392(1)	Khosrov reserve, Ararat prov., Mangyuz env. (Armenia)	JQ045176	JQ045242			
311	MCC R1392(2)	Khosrov reserve, Ararat prov., Mangyuz env. (Armenia)	JQ045176	JQ045242			
312	MCC R1392(3)	Khosrov reserve, Ararat prov., Mangyuz env. (Armenia)	JQ045176	JQ045242			
313	MCC R1392(4)	Khosrov reserve, Ararat prov., Mangyuz env. (Armenia)	JQ045176	JQ045242	MT773919	MT773984	MT774045
314	MCC R1363	Nagorno Karabakh, Hadrut prov., Azokhk (Azerbaijan)	JQ045176	JQ045242	MT773920	MT773985	JQ045263
316	MCC R1364	Vayots Dzor prov., Noravank (Armenia)	JQ045176	JQ045242			
317	MCC R1261	Khosrov reserve, Ararat prov., Mangyuz env. (Armenia)	JQ045176	JQ045242	MT773921	MT773986	JQ045263
320	NMP6V 70460-1	4 km E of Sweida (Syria)	JQ045177	JQ045243	MT773922	MT773987	MT774046
321	NMP6V 70460-2	4 km E of Sweida (Syria)	JQ045178	JQ045244	MT773923	MT773988	JQ045264
324	NMP6V 72075-1	Ermones, Kerkira Island (Greece)	JQ045179	JQ045245	MT773924	MT773989	JQ045263
325	NMP6V 72075-2	Ermones, Kerkira Island (Greece)	JQ045179	JQ045245			
326	NMP6V 72540	Al´Adimah, 5 km S of Baniyas, Al´Adimah (Syria)	JQ045180	JQ045246	MT773925	MT773990	MT774047
327	NMP6V 72541	Gecitköy (Cyprus)	JQ045181	JQ045247			
328	NMP6V 72685	Cincevat River, Tuzluca (Turkey)	JQ045182	JQ045248	MT773926	MT773991	JQ045263
332		Achladokampos (Greece)	JQ045183	JQ045249			
333		Ptelea (Greece)	JQ045184	JQ045250			
334		Kremaston Lake (Greece)	JQ045172	JQ045238			

335		Kremaston Lake (Greece)	JQ045172	JQ045238			
336	ZDEU 2a	Polateli, Kilis (Turkey)	JQ045185	JQ045251			
337	ZDEU 3a	16 km SE of Halfeti, Şanlıurfa (Turkey)	JQ045172	JQ045238	MT773927	MT773992	JQ045263
338	ZDEU 4a	Küçükalanlı, 10 km W of Şanlıurfa, Şanlıurfa (Turkey)	JQ045186	JQ045252			
339	ZDEU 5a	Yapağlı, Çivril, Denizli (Turkey)	JQ045187	JQ045253			
340	ZDEU 6a	Between Aydıncık and Gülnar, Mersin (Turkey)	JQ045188	JQ045254			
341	ZDEU 6b	Between Aydıncık and Gülnar, Mersin (Turkey)	JQ045189	JQ045255	MT773928	MT773993	JQ045263
342	ZDEU 6c	Between Aydıncık and Gülnar, Mersin (Turkey)	JQ045189	JQ045255			
343	ZDEU 6d	Between Aydıncık and Gülnar, Mersin (Turkey)	JQ045189	JQ045255			
344	ZDEU 6e	Between Aydıncık and Gülnar, Mersin (Turkey)	JQ045189	JQ045255			
345	ZDEU 7a	20 km N of Derebucak, Beyşehir, Konya (Turkey)	JQ045172	JQ045238			
346	ZDEU 8a	Akdağ, Çivril, Denizli (Turkey)	JQ045172	JQ045238	MT773929	MT773994	JQ045263
347	ZDEU 9a	Eğirdir, Isparta (Turkey)	JQ045190	JQ045256	MT773930	MT773995	MT774048
348	ZDEU 9b	Eğirdir, Isparta (Turkey)	JQ045149	JQ045215	MT773931	MT773996	JQ045263
349	ZDEU 9c	Eğirdir, Isparta (Turkey)	JQ045190	JQ045256			
350	ZDEU 10a	27 km N of Akseki, Antalya (Turkey)	JQ045191	JQ045257	MT773932	MT773997	JQ045263
351	ZDEU 11a	Between Polatlı and Haymana, Ankara (Turkey)	JQ045192	JQ045258	MT773933	MT773998	JQ045263
352	ZDEU 12a	Between Simav and Demirci, Kütahya (Turkey)	JQ045193	JQ045259	MT773934	MT773999	MT774049
353	ZDEU 12b	Between Simav and Demirci, Kütahya (Turkey)	JQ045194	JQ045260			
354	ZDEU 13a	Between Gündoğmuş and Akseki, Antalya (Turkey)	JQ045195	JQ045261			
360	ZDEU 1a	Yayladağ, Hatay (Turkey)	JQ045196	JQ045262	MT773935	MT774000	JQ045274
361		Guzelyali (Turkey)	MT773683	MT773798			
362		Guzelyali (Turkey)	MT773684	MT773799			
363		Guzelyali (Turkey)	MT773685	MT773800			
364		Guzelyali (Turkey)	MT773686	MT773801			
365		Guzelyali (Turkey)	MT773687	MT773802			
366		Guzelyali (Turkey)	MT773688	MT773803			
367		Oymapinar (Turkey)	MT773689	MT773804			
368		Oymapinar (Turkey)	MT773690	MT773805			
369		Oymapinar (Turkey)	MT773691	MT773806			
370		Oymapinar (Turkey)	MT773692	MT773807			
371		Oymapinar (Turkey)	MT773693	MT773808			
372		Oymapinar (Turkey)	MT773694	MT773809			
373		Oymapinar (Turkey)	MT773695	MT773810			
374		Ucoluk, southwest Antalya (Turkey)	MT773696	MT773811			
375		Ucoluk, southwest Antalya (Turkey)	MT773697	MT773812			
376		Ucoluk, southwest Antalya (Turkey)	MT773698	MT773813			
377		Ucoluk, southwest Antalya (Turkey)	MT773699	MT773814			
378		Ucoluk, southwest Antalya (Turkey)	MT773700	MT773815			
379		Near Emecik (Turkey)	MT773701	MT773816			
380		Near Emecik (Turkey)	MT773702	MT773817			
381		Near Avsalar (Turkey)	MT773703	MT773818	MT773936	MT774001	MT774050
382		North Bektas (Turkey)	MT773704	MT773819	MT773937	MT774002	MT774051
383		North Bektas (Turkey)	MT773705	MT773820	MT773938	MT774003	MT774052
384		Outside Ulupinar (Turkey)	MT773706	MT773821			
385		North Yuvalilar (Turkey)	MT773707	MT773822	MT773939	MT774004	MT774053
387		Telmessos castle (Turkey)	MT773708	MT773823			
388		Telmessos castle (Turkey)	MT773709	MT773824			
389		Termessos (Turkey)	MT773710	MT773825	MT773940	MT774005	MT774054
390		Termessos (Turkey)	MT773711	MT773826	MT773941	MT774006	MT774055
391		west of Mergenli (Turkey)	MT773712	MT773827	MT773942	MT774007	MT774056
392	ZDEU 392/2011	Silopi, Sirnak, Salih Ladus (Turkey)	MT773713	MT773828			
393	ZDEU 393/2011	Silopi, Sirnak, Salih Ladus (Turkey)	MT773714	MT773829	MT773943	MT774008	MT774057
394	ZDEU 394/2011	Oualihi kemalpasa, Izmir (Turkey)	MT773715	MT773830	MT773944	MT774009	MT774058
395	ZDEU 395/2011	Oualihi kemalpasa, Izmir (Turkey)	MT773716	MT773831			
396	ZDEU 396/2011	Meydandere (Turkey)	MT773717	MT773832	MT773945	MT774010	MT774059
397	ZDEU 397/2011	Meydandere (Turkey)	MT773718	MT773833			
398	ZDEU 398/2011	Nizip Gaziantep (Turkey)	MT773719	MT773834	MT773946	MT774011	MT774060
399	ZDEU 399/2011	Siirt (Turkey)	MT773720	MT773835	MT773947	MT774012	MT774061
400	ZDEU 400/2011	Cirali (Turkey)	MT773721	MT773836			
401		Kale castle (Turkey)	MT773722	MT773837			
402		Kale castle (Turkey)	MT773723	MT773838			
403		Kale castle (Turkey)	MT773724	MT773839			
404		Geyre (Turkey)	MT773725	MT773840			
405		Geyre (Turkey)	MT773726	MT773841			
406		Geyre (Turkey)	MT773727	MT773842	MT773948	MT774013	MT774062
407		Geyre (Turkey)	MT773728	MT773843			
408		Kızılcaağaç (Turkey)	MT773729	MT773844	MT773949	MT774014	MT774063
409		2 km North Hasanpaşa (Turkey)	MT773730	MT773845	MT773950	MT774015	MT774064
410		2 km North Hasanpaşa (Turkey)	MT773731	MT773846			
411		2 km North Hasanpaşa (Turkey)	MT773732	MT773847			

412		2 km North Hasanpaşa (Turkey)	MT773733	MT773848			
413		2 km North Hasanpaşa (Turkey)	MT773734	MT773849			
414		North of lake Agkol (Turkey)	MT773735	MT773850			
415		North of lake Agkol (Turkey)	MT773736	MT773851			
416		North of lake Agkol (Turkey)	MT773737	MT773852			
417		mount Karaman (Turkey)	MT773738	MT773853	MT773951	MT774016	MT774065
418		Uzuncaburç (Turkey)	MT773739	MT773854	MT773952	MT774017	MT774066
419		Uzuncaburç (Turkey)	MT773740	MT773855			
420		Zeyne (Turkey)	MT773741	MT773856			
421		Zeyne (Turkey)	MT773742	MT773857			
422		Bozagac (Turkey)	MT773743	MT773858			
423		Alahan Monastery (Turkey)	MT773744	MT773859	MT773953	MT774018	MT774067
424		Kayrak (Turkey)	MT773745	MT773860			
432	AAMU TV5A	İncesu (Turkey)	MT773746	MT773861			
433	AAMU TV5B	İncesu (Turkey)	MT773747	MT773862			
434	AAMU TV6A	Şırnak (Turkey)	MT773748	MT773863	MT773954	MT774019	MT774068
435	AAMU TV9A	Sofular (Turkey)	MT773749	MT773864	MT773955	MT774020	MT774069
436	AAMU TV10A	Yayladağ (Turkey)	MT773750	MT773865	MT773956	MT774021	MT774070
437	AAMU TV11A	Reyhanlı-Kırıkhan (Turkey)	MT773751	MT773866	MT773957	MT774022	MT774071
438	AAMU TV12A	Olgunlar (Turkey)	MT773752	MT773867	MT773958	MT774023	MT774072
439	AAMU TV12B	Olgunlar (Turkey)	MT773753	MT773868			
440	AAMU TV14A	Hanağzı-Islahiye (Turkey)	MT773754	MT773869			
441	AAMU TV15A	25 km N of Adıyaman (Turkey)	MT773755	MT773870			
442	AAMU TV15B	25 km N of Adıyaman (Turkey)	MT773756	MT773871	MT773959	MT774024	MT774073
443	AAMU TV17A	Yeniköy-Çine (Turkey)	MT773757	MT773872	MT773960	MT774025	MT774074
444	AAMU TV17B	Yeniköy-Çine (Turkey)	MT773758	MT773873			
445	AAMU TV18A	Yuvabaşı (Turkey)	MT773759	MT773874			
446	AAMU TV18B	Yuvabaşı (Turkey)	MT773760	MT773875			
447	AAMU TV19A	Topbağalı (Turkey)	MT773761	MT773876	MT773961	MT774026	MT774075
448	AAMU TV19B	Topbağalı (Turkey)	MT773762	MT773877			
449	AAMU TV19C	Topbağalı (Turkey)	MT773763	MT773878			
450	AAMU TV19D	Topbağalı (Turkey)	MT773764	MT773879			
451	AAMU TV20A	Kozan (Turkey)	MT773765	MT773880	MT773962	MT774027	MT774076
452	AAMU TV20B	Kozan (Turkey)	MT773766	MT773881			
453	AAMU TV20C	Kozan (Turkey)	MT773767	MT773882			
454	AAMU TV21A	Küplüce (Turkey)	MT773768	MT773883			
455	AAMU TV22A	Uzunali (Turkey)	MT773769	MT773884	MT773963	MT774028	MT774077
456	AAMU TV23A	Feke (Turkey)	MT773770	MT773885	MT773964	MT774029	MT774078
457	AAMU TV24A	Ayransuyu (Turkey)	MT773771	MT773886	MT773965	MT774030	MT774079
458	AAMU TV24B	Ayransuyu (Turkey)	MT773772	MT773887			
459	AAMU TV25A	Mürşitpınar (Turkey)	MT773773	MT773888			
460	AAMU TV25B	Mürşitpınar (Turkey)	MT773774	MT773889			
462	AAMU TV26B	Elbeyli (Turkey)	MT773775	MT773890			
463	AAMU TV26C	Elbeyli (Turkey)	MT773776	MT773891	MT773966	MT774031	MT774080
465	AAMU TV26E	Elbeyli (Turkey)	MT773777	MT773892			
466	AAMU TV27A	Höyük (Turkey)	MT773778	MT773893	MT773967	MT774032	MT774081
467	AAMU TV28A	Pozantı (Turkey)	MT773779	MT773894			
468	AAMU TV28B	Pozantı (Turkey)	MT773780	MT773895			
469	AAMU TV28C	Pozantı (Turkey)	MT773781	MT773896	MT773968	MT774033	MT774082
470	AAMU TV28D	Pozantı (Turkey)	MT773782	MT773897			
471	AAMU TV29A	Yukarı (Turkey)	MT773783	MT773898			
472	AAMU TV29B	Yukarı (Turkey)	MT773784	MT773899			
473	AAMU TV29C	Yukarı (Turkey)	MT773785	MT773900			
474	AAMU TV30A	Suçeğin – Arguvan (Turkey)	MT773786	MT773901	MT773969	MT774034	MT774083
477		Strofylia (Greece)	MT773787	MT773902	MT773970	MT774035	MT774084
478		Argolida (Greece)	MT773788	MT773903			
479		Yliki (Greece)	MT773789	MT773904	MT773971	MT774036	MT774085
480	TAU-R 16214	Upper Galil (Israel)	MT773790	MT773905			
481	TAU-R 16698	Shomeron Malkishua' (Israel)	MT773791	MT773906	MT773972	MT774037	MT774086
482	NMP6V 70460-3	4 km E of Sweida (Syria)	MT773792	MT773907			
6795	CUB 6795	Houch Aammiq (Lebanon)	MT773793	MT773908	MT773974	MT774039	MT774088
6796	CUB 6796	Houch Aammiq (Lebanon)	MT773794	MT773909	MT773975	MT774040	MT774089
6797	CUB 6797	Houch Aammiq (Lebanon)	MT773795	MT773910	MT773976	MT774041	MT774090
6798	CUB 6798	Houch Aammiq (Lebanon)	MT773796	MT773911	MT773977	MT774042	MT774091
8986	CUB 8986	Paphos (Cyprus)	MT773797	MT773912	MT773973	MT774038	MT774087

Figure S3

Summary of the bGMYC results. On the left: the maximum clade credibility tree of our mtDNA phylogeny. On the right: a heat map depiction of the matrix of pairwise posterior probabilities of conspecificity (colour scale at the far right of the figure).

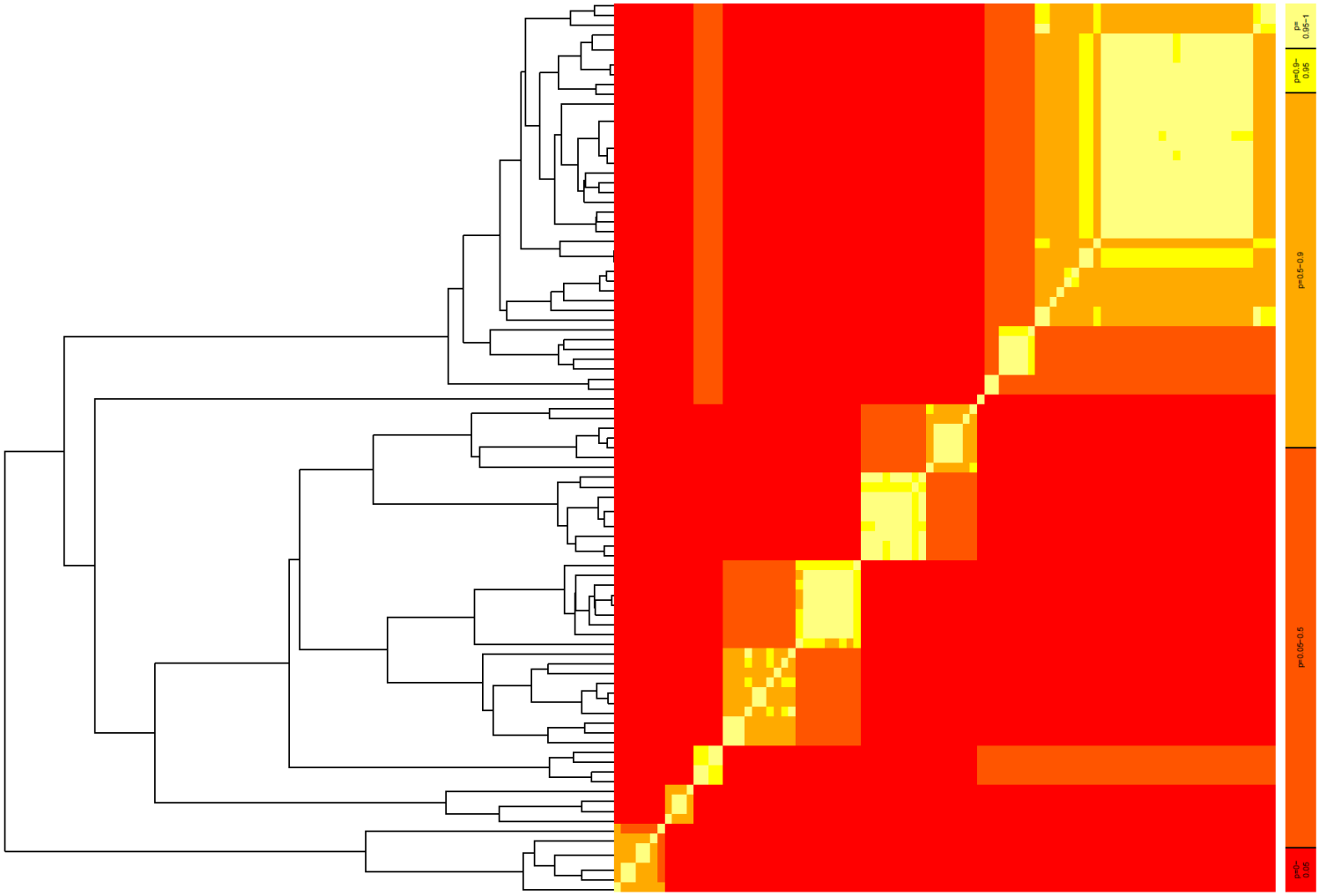

Figure S4

The species tree inferred with the application of STACEY in BEAST2. Terminal nodes refer to the "species", i.e. the maximum number of mtDNA clusters estimated from the combination of all single-locus species delimitation analyses (13 species). Numbers next to nodes are posterior probabilities.

Figure S5. The illustrations form Jan (1864) describing the holotype of *Xerotyphlops syriacus*, with specific morphological features.

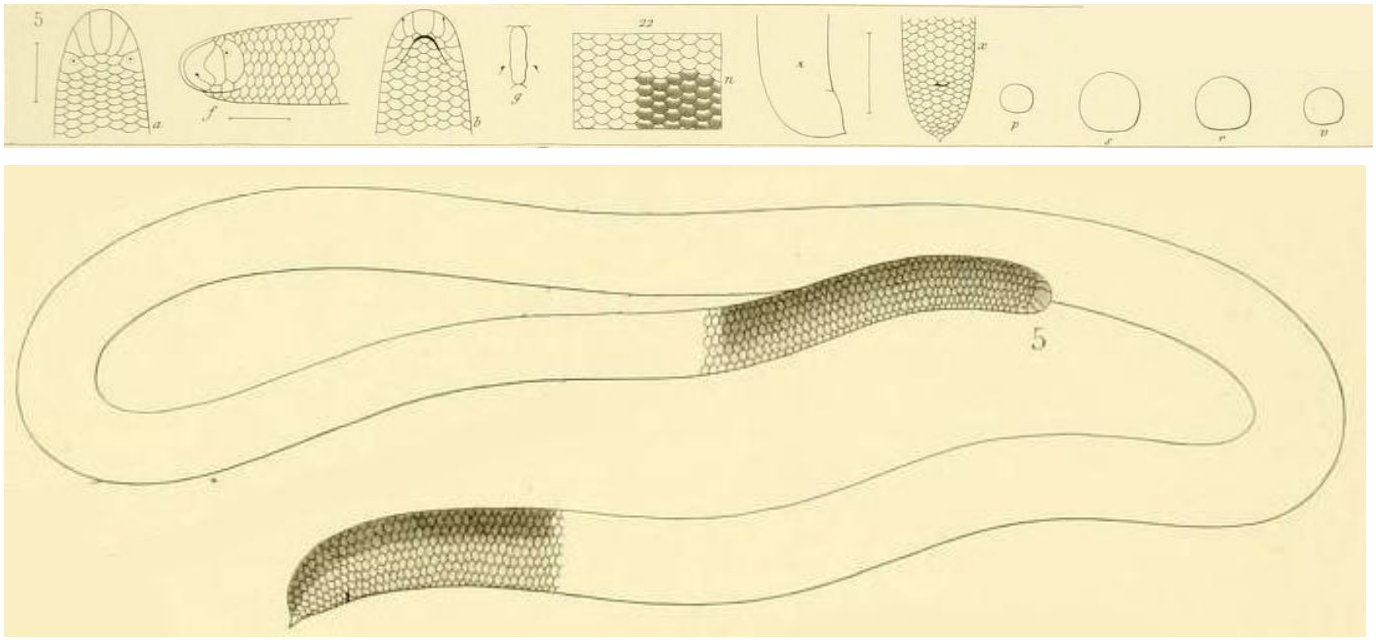

Table S6. Mean genetic divergences (% p-distance values) among major mtDNA groups for ND2 and 12S. Values on the diagonal are genetic divergences within each group. For group abbreviations, see Figs. 1 and 2.

ND2

Major Groups	A	B	C	D	E	F	G	K	IHM
A	3.4								
B	13.0	0.4							
C	10.6	6.7	0.4						
D	12.1	7.8	5.2	0.9					
E	11.3	7.0	3.0	4.7	0.2				
F	11.7	7.9	4.3	5.5	4.3	-			
G	11.5	7.0	4.3	5.9	3.5	4.8	0.5		
K	11.7	7.4	3.9	5.6	3.7	4.5	3.5	1.3	
IHM	11.3	8.3	4.2	5.8	2.9	4.3	4.3	3.9	0.5

12S

Major Groups	A	B	C	D	E	F	G	K	IHM
A	1.3								
B	5.0	0.1							
C	4.8	2.4	0.1						
D	5.7	3.4	3.4	0.8					
E	4.8	3.3	2.6	3.1	0.1				
F	4.4	3.9	3.7	3.2	1.5	-			
G	4.9	3.0	2.8	2.6	2.3	2.9	0.2		
K	5.2	3.6	3.3	2.9	2.8	3.4	1.0	0.4	
IHM	5.2	2.7	2.5	3.4	2.0	2.6	2.1	2.2	0.2

References

Jan, G., 1864. Iconographie générale des ophidiens. 3. Livraison. Iconogr. gén. Ophid., 1 (3. livr.): 3.

Kornilios, P., Ilgaz, H., Kumlutas, Y., Lymberakis, P., Moravec, J., Sindaco, R., Rastegar-Pouyani, N., Afroosheh, M., Giokas, S., Fraguedakis-Tsolis, S., Chondropoulos, B., 2012. Neogene climatic oscillations shape the biogeography and evolutionary history of the Eurasian blindsnake. Mol. Phylogenet. Evol. 62, 856–873.

Vitt, L.J., Caldwell., J.P., 2014. Herpetology. An Introductory Biology of Amphibians and Reptiles. Fourth Edition. Amsterdam: Elsevier.